# Estimating Time-Varying Nonlinear Autoregressive Model Parameters by Minimizing Hypersurface Distance

Bufan Yang and Ki H. Chon*, *Senior Member, IEEE*

***Abstract*—A nonleast-squares (non-LS) based method is presented for modeling time-varying (TV) nonlinear systems. The proposed method combines basis function technique and minimization of hypersurface distance (MHD) to combat TV and nonlinear dynamics, respectively. The performance of TVMHD is compared to the LS and total LS methods using simulation examples as well as human heart rate data recorded during different body positions. With all data, TVMHD significantly outperforms the two other methods by a factor of one order of magnitude; the LS-based methods require double the number of parameters than TVMHD requires to obtain similar residual error values. The significance of TVMHD is that due to its accurate parameter estimates concomitant with a fewer number of parameters, we now have the possibility of pinpointing parameters that may be of physiological importance, where such application will be especially useful in discriminating diseased conditions. Furthermore, our algorithm allows discrimination of model terms, which are TV or time invariant, by examining those basis function coefficients that are designed to capture TV dynamics. However, it should be noted that the main disadvantage of TVMHD is that it requires significantly greater computational time than the LS-based methods.**

***Index Terms*—Basis function, heart rate variability (HRV), nonlinear autoregressive moving average (ARMA) models, nonstationary signal, time varying (TV).**

## I. Introduction

Most physiological signals exhibit nonlinear and time-varying (TV) dynamics [1]. However, algorithms available to handle identification of nonlinear and TV signals have been limited in the literature for a myriad of reasons [2]. For example, the combined effect of nonlinearity and TV dynamics leads to significant increase in the number of model parameters to be estimated. Further, sudden changes in the dynamics of the signal also pose significant challenges, as most TV techniques are mainly effective for slow TV signals.

Recent parametric approaches have begun to tackle signals that exhibit both nonlinear and nonstationary dynamics. A work by Faes *et al.* is noteworthy because it combines the $k$-nearest neighbor local linear approximation and an expansion of model parameters onto a set of predefined basis functions to handle both nonlinearity and nonstationarity in the data [3]. Most algorithms for parameter estimation of linear and nonlinear autoregressive moving average (ARMA) models involve the least-squares (LS) approach, including the aforementioned method by Faes *et al.* [3]. However, the limitations of the LS-based techniques for parameter estimation are well documented and their performance suffers because of what is known as the error-in-variables problem [4]. Specifically, the LS assume that only the observation vector, and not the candidate matrix, is perturbed by the noise source. The LS solution is unbiased only when the candidate matrix is clean, and if not, it results in the error-in-variables problem. A time-invariant (TIV) nonlinear ARMA method that overcomes the error-in-variables problem especially for nonlinear parameter estimation by minimizing the total summed distance over a hypersurface has been proposed [5]. The technique, known as the minimization of hypersurface distance (MHD), significantly outperformed both the LS and total LS (TLS) in a variety of simulation examples consisting of different noise sources (e.g., white or colored noise that is either additive or dynamic). MHD incorporates both the optimal parameter search (OPS) criterion [6] for accurate model-order selection and an initial parameter estimation using the TLS method. The TLS method was used for parameter estimation because it partly overcomes the error-in-variables problem of the LS. Once the initial parameter estimates are obtained, they are further optimized using the MHD approach. Due to these various procedures, the main limitation of the MHD is the significant increase in the computation time as compared to the LS; therefore, it is mainly suitable for systems that can be characterized by only a few parameters.

Our motivation for developing an accurate parameter-estimation technique stems from the fact that a physiologically interpretable model requires a compact system representation. For such a compact system, few parameters are a must. The LS-based parameter-estimation techniques have not been able to achieve a compact system representation because many parameters are needed to reduce the MSE to a meaningfully low value. This limitation of the LS-based approaches can be surmounted by TVMHD, as it will be shown in the Section III that equally accurate system representation can be obtained even with only half the number of parameters. With a small number of parameters, we will have an opportunity to ask important questions, such as

Manuscript received September 21, 2009; revised December 23, 2009, February 3, 2010 and March 3, 2010; accepted March 5, 2010. Date of publication May 17, 2010; date of current version July 14, 2010. This work was supported in part by the Office of Naval Research Work Unit under Grant N00014-08-1-0244. *Asterisk indicates corresponding author.*

B. Yang is with the Department of Biomedical Engineering, Worcester Polytechnic Institute, Worcester, MA 01609 USA (e-mail: bf@wpi.edu).

*K. H. Chon is with the Department of Biomedical Engineering, Worcester Polytechnic Institute, Worcester, MA 01609 USA (e-mail: kichon@wpi.edu).

Digital Object Identifier 10.1109/TBME.2010.2045377

which parameters may be linked to the dynamics pertaining to diseased conditions.

Given the significant improvement in the accuracy of parameter estimation of the MHD compared to either the LS or TLS, the aim of this paper was to extend the algorithm to be applicable for TV nonlinear signals. An approach we have taken is to expand the TV parameters onto a set of basis functions, which has been shown to provide good results in tracking both slow and relatively fast transient dynamics [7]. Both computer simulation examples and application of the new proposed method to heart rate variability (HRV) data are provided to illustrate the feasibility of the proposed method. Further, comparison of the TVMHD to TVLS and TVTLS are provided.

## II. Methods

Consider a nonlinear TVARMA model

$$\begin{aligned} y(n) = &\sum_{i=1}^{P} a(i,n)\, y(n-i) + \sum_{j=1}^{Q} b(j,n)\, x(n-j) + \cdots \\ &+ \sum_{i=1}^{P}\sum_{j=1}^{P} c(i,j,n)\, y(n-i)\, y(n-j) + \cdots \\ &+ \sum_{i=1}^{Q}\sum_{j=1}^{Q} d(i,j,n)\, x(n-i)\, x(n-j) + \cdots \\ &+ \cdots + e(n) \end{aligned} \tag{1}$$

where $a(i,n)$ and $b(j,n)$ are the TV AR and MA coefficients, respectively, and $c(i,j,n)$ and $d(i,j,n)$ are the TV nonlinear AR and MA coefficients, respectively. The superscripts $P$ and $Q$ are the maximum AR and MA model orders, respectively, and $e(n)$ is the prediction error. Any of the parameter-estimation techniques, such as the TVOPS [6], [8], TVTLS, or the proposed TVMHD can be used to solve for the unknown linear and nonlinear TV ARMA parameters in (1). Fig. 1 provides succinct graphical representations of the differences between the LS, TLS, and MHD approaches. TV representations of LS and TLS are provided elsewhere [1]; therefore, we only provide detailed description of the TVMHD. It should be noted that for linear systems, the MHD is essentially identical to TLS. To illustrate the concept of the TVMHD approach, consider a three-term TV nonlinear AR model

$$y(n) = a(1,n)\, y(n-1) + c(2,2,n)\, y^2(n-2) + e(n). \tag{2}$$

The system of (2) is solved by expanding the TV coefficients onto a set of basis functions $\pi_k$ such that

$$\begin{aligned} y(n) = &\sum_{i=1}^{P}\sum_{k=0}^{V} \alpha(i,k)\, \pi_k(n)\, y(n-1) \\ &+ \sum_{i=1}^{P}\sum_{j=1}^{P}\sum_{k=0}^{V} \alpha(i,j,k)\, \pi_k(n)\, y(n-i)\, y(n-j) \\ &+ e(n) \end{aligned} \tag{3}$$

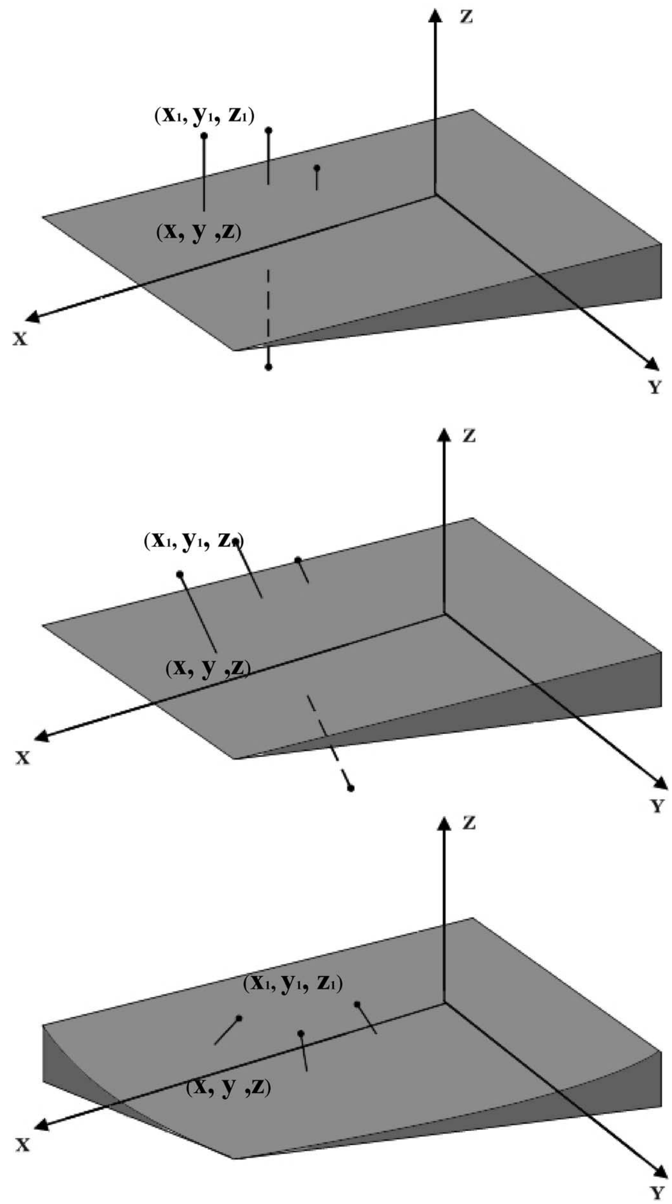


Fig. 1. Graphical representation of the distance minimization solutions of (top) TVOPS, (middle) TVTLS, and (bottom) TVMHD.

where $\alpha(i,k)$ and $\alpha(i,j,k)$ represent the linear and nonlinear expansion parameters, respectively, with $V+1$ as the maximum number of basis sequences [1]. If $V$ is selected to be 1 and $\alpha(i,k) = \alpha_{ik}$, for simplicity, we have

$$\begin{aligned} y(n) = &\alpha_{10}\pi_0(n)\, y(n-1) + \alpha_{11}\pi_1(n)\, y(n-1) \\ &+ \alpha_{220}\pi_0(n)\, y(n-2)^2 + \alpha_{221}\pi_1(n)\, y(n-2)^2. \end{aligned} \tag{4}$$

For simplicity, with $y(n) = z$, $y(n-1) = x$, and $y(n-2) = y$, the aforementioned equation could be rewritten as follows:

$$z = \alpha_{10}\pi_0 x + \alpha_{11}\pi_1 x + \alpha_{220}\pi_0 y^2 + \alpha_{221}\pi_1 y^2. \tag{5}$$

The cost function is to minimize the following:

$$\min_{\alpha_{1k},\alpha_{22k}} \left( \sum_{i=1}^{N} \min((z - z_i)^2 + (x - x_i)^2 + (y - y_i)^2) \right), \quad k = 0, 1. \tag{6}$$

By substituting $z$ from (5) into (6), we find the following:

$$\begin{aligned} f(\alpha_{1k}, \alpha_{22k}, x, y) = {} & \left(\alpha_{10}\pi_0 x + \alpha_{11}\pi_1 x + \alpha_{220}\pi_0 y^2 \right. \\ & \left. + \alpha_{221}\pi_1 y^2 - z_i\right)^2 \\ & + \left(x - x_i^2\right) + (y - y_i)^2 \end{aligned} \tag{7}$$

$$\begin{aligned} & \frac{\partial f(\alpha_{1k}, \alpha_{22k}, x, y)}{\partial x} = 0 \\ & \left(\alpha_{10}\pi_0 x + \alpha_{11}\pi_1 x + \alpha_{220}\pi_0 y^2 + \alpha_{221}\pi_1 y^2 - z_i\right) \\ & \quad \times (\alpha_{10}\pi_0 + \alpha_{11}\pi_1) + (x - x_i) = 0 \end{aligned} \tag{8}$$

$$\begin{aligned} & \frac{\partial f(\alpha_{1k}, \alpha_{22k}, x, y)}{\partial x} = 0 \\ & 2\left(\alpha_{10}\pi_0 x + \alpha_{11}\pi_1 x + \alpha_{220}\pi_0 y^2 + \alpha_{221}\pi_1 y^2 - z_i\right) \\ & \quad \times (\alpha_{220}\pi_0 y + \alpha_{221}\pi_1 y) + (y - y_i) = 0. \end{aligned} \tag{9}$$

Equations (8) and (9) are solved for $x$ and $y$, followed by $z$ via (5). The solution is the point on the hypersurface (in this case the 3-D surface, as defined by $x$, $y$, and $z$) that is closest to the data point $(x_i, y_i, z_i)$. By substituting the computed $x$, $y$, and $z$, the corresponding distance is obtained from the cost function in (7). Subsequently, we set $g(\alpha_{1k}, \alpha_{22k}) = \min(f(\alpha_{1k}, \alpha_{22k}, x, y))$, and obtain coefficients that minimize the total distance by computing partial derivatives as follows:

$$\begin{aligned} & \min\left(\sum_{i=1}^{N} g(\alpha_{1k}, \alpha_{22k})\right) \frac{\partial \sum_{i=1}^{N} g(\alpha_{1k}, \alpha_{22k})}{\partial \alpha_{1k}} = 0, \\ & \qquad k = 0, 1. \\ & \frac{\partial \sum_{i=1}^{N} g(\alpha_{1k}, \alpha_{22k})}{\partial \alpha_{22k}} = 0 \end{aligned} \tag{10}$$

If the dimension of the system is less than or equal to three, the analytical solution that minimizes the cost function can be obtained in most cases. In practice, the analytical solution of (10) is difficult to obtain when the hypersurface has a complex function. Thus, a numerical solution is obtained using a search method. Initially, we set a range of values for the parameters $\alpha_{1k}$ and $\alpha_{22k}$ with initial values of these parameters obtained from the TVOPS method [6], [8], such that (8) and (9) are minimized using the Frobenius norm. Note that for every value of $\alpha_{1k}$ and $\alpha_{22k}$, a new hypersurface is created, a minimum Euclidean distance is found, and these values are then summed to produce the total distance. The values of parameters $\alpha_{1k}$ and $\alpha_{22k}$ that produce the minimum total summed distance are selected to be the best-estimated choice of parameters. The performance metric that we have used to compare the three methods is the normalized MSE (NMSE) values.

### A. Simulation Examples

For all simulation examples, we considered the following TV nonlinear AR model, where "$a$" is the TV parameter

$$\begin{aligned} y(n) = {} & -0.5y(n-1) + ay(n-1)^2 - 0.65y(n-2) + \cdots \\ & + 0.5y(n-3) + e(n). \end{aligned} \tag{11}$$

For all simulation examples, 1024 data points were generated. Due to the fact that the MHD method is a numerical search method, it is not sensitive to the length of data samples, and we have verified that data samples as small as 300 and as large as 2000 did not affect the results. For all simulation examples, 20 independent realizations of Gaussian white noise (GWN) were generated. The variance of GWN was adjusted so that when it was added to the 1024 datapoint series, the SNR was 10 dB.

### B. Experimental Data Collection

Six healthy people (20–40 years old) participated in the experiment. Measurements of ECG data sampled at 500 Hz were collected during the following conditions: 1) supine position, 2) transition data from the supine to upright position, and 3) upright position. The QRS complexes in the ECG were used to identify beat locations. Once the timing of beats was determined, an instantaneous heart rate (HR) signal was created at a sampling rate of 4 Hz using the cubic interpolation. Each HR dataset contained 300 data points, which is equivalent to 1.25 min. All data were demeaned and normalized to unit variance for each subject. To evaluate these algorithms' performance on data with different postures (supine versus upright) and nonstationary conditions (transition state from the supine to upright positions), tilt table experiments were performed. Experiments were first performed in the supine position for 10 min, followed by raising the tilt table to the upright (80° tilt) position. There was 1–2 min of transition from the supine to upright position and the data were collected for an additional 10 min in the upright position. Data recordings were not interrupted during the transition between the two body positions.

For TV analyses involving both TVMHD and TVOPS methods, an initial model order of six linear and six second-order nonlinear terms were selected. We also investigated two different selections of basis functions: 1) four Legendre and two Walsh and 2) four Legendre and four Walsh. We did not compare TVTLS to TVMHD and TVOPS with the experimental data, since the simulation examples shown in the Section III clearly indicate its poor performance.

## III. Results

To demonstrate the efficacy of the TVMHD method, we perform both simulation examples and application to human HRV data. For both cases, we compare the performance of TVMHD to TVOPS and TVTLS methods. Note that the TVOPS is based on the LS approach; therefore, we have used TVOPS as a representative method for TVLS. We chose TVOPS because it has been shown to provide accurate model terms despite incorrect *a priori* model-order selection [6].

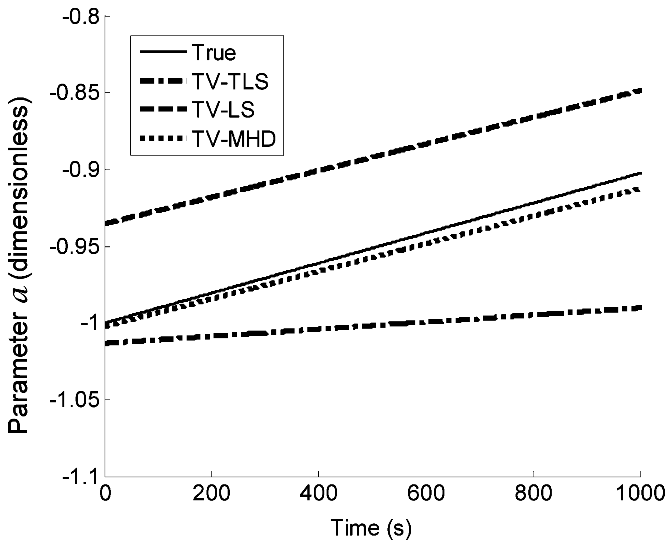


Fig. 2. Estimated value of the TV parameter "a" using the TVTLS, TVOPS, and TVMHD methods when "a" in (11) linearly increases over time.

TABLE I
TIV COEFFICIENT ESTIMATES VIA TVOPS, TVTLS, AND TVMHD FOR SIMULATION EXAMPLE 1

| AR Model Coefficients for model terms: | AR Terms | | |
|---|---|---|---|
| | **y(n-1)** | **y(n-2)** | **y(n-3)** |
| True value | -0.5 | -0.65 | 0.5 |
| TVOPS | -0.473±0.067 | -0.619±0.035 | 0.536±0.036 |
| TVTLS | -0.649±0.190 | -0.722±0.089 | 0.425±0.099 |
| TVMHD | -0.511±0.035 | -0.660±0.081 | 0.480±0.005 |

## A. Simulation Results

For the first simulation example, the TV coefficient "$a$" increases linearly, as shown by the solid line in Fig. 2. The initial model orders were set to $L = 8$ linear AR lags, $N = 4$ nonlinear AR lags, and $V = 1$ Legendre basis function. This resulted in $[L + N(N + 1)/2](V + 1) = 36$ candidate terms in total. We selected $V = 1$ Legendre basis function based on the MSE criterion [1]. Despite this overdetermined model-order selection, the OPS correctly selected three linear and one nonlinear term out of the 36 candidates. Comparison of time TIV coefficients of (11), represented as the mean and standard deviation via TVOPS, TVTLS, and TVMHD, are shown in Table I. The estimates of the TV parameter "$a$" are shown in Fig. 2. The dotted, dashed, and dash–dotted lines represent TVMHD, TVOPS, and TVTLS, respectively. Comparison of the three methods' performance, as determined by the NMSE, is shown in the second column of Table II. Coefficient estimates for both TV and TIV parameters are the most accurate for the TVMHD, followed by TVOPS and TVTLS. The NMSE value for the MHD is significantly lower than both TVOPS and TVTLS by a factor of 2.6 and 7.9, respectively.

TABLE II
NMSE VALUES FOR TVOPS, TVTLS, AND TVMHD FOR THREE SIMULATION EXAMPLES

| NMSE | **Simulation 1** | **Simulation 2** | **Simulation 3** |
|---|---|---|---|
| TVOPS | 0.208±0.028 * | 0.459 ± 0.033 * | 0.223± 0.051 * |
| TVTLS | 0.621±0.057 | 0.909 ± 0.109 | 0.895±0.071 |
| TVMHD | 0.078±0.008 | 0.047 ± 0.011 | 0.061±0.017 |

*Denotes that the three methods are significantly different from each other ($p < 0.01$).

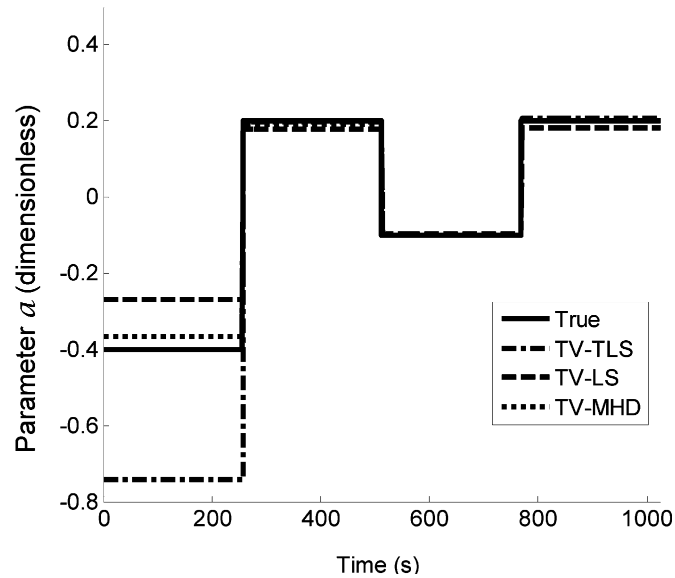


Fig. 3. Estimated value of the TV parameter "a" using the TVTLS, TVOPS, and TVMHD methods when "a" in (11) changes abruptly over time.

TABLE III
TIV COEFFICIENT ESTIMATES VIA TVOPS, TVTLS, AND TVMHD FOR SIMULATION EXAMPLE 2

| AR Model Coefficients | AR Terms | | |
|---|---|---|---|
| | **y(n-1)** | **y(n-2)** | **y(n-3)** |
| True value | -0.5 | -0.65 | 0.5 |
| TVOPS | -0.358±0.160 | -0.606±0.029 | 0.557±0.045 |
| TVTLS | -0.651±0.173 | -0.754±0.112 | 0.370±0.072 |
| TVMHD | -0.520±0.101 | -0.633±0.049 | 0.465±0.057 |

The second simulation example examines the responses of the methods when the TV parameter "$a$" undergoes a fast change, as shown in Fig. 3. Similar to the previous simulation example, TVMHD yields the most accurate estimate for both TIV and TV coefficients; comparison of NMSE values for all three methods are shown in the third column of Table II. The NMSE value for TVMHD is less than that of the TVOPS and TVTLS approaches by a factor of 10 and 20, respectively. Despite 10 dB additive noise in all three simulation examples, both TIV and TV coefficient estimates obtained by TVMHD do not deviate much from the true values, whereas they do for both TVOPS and TVTLS methods (see Table III).

The third simulation example is based on (11) with the TV coefficient "$a$" changing with the parabolic shape, shown in Fig. 4, is represented by the solid line. For this example, the

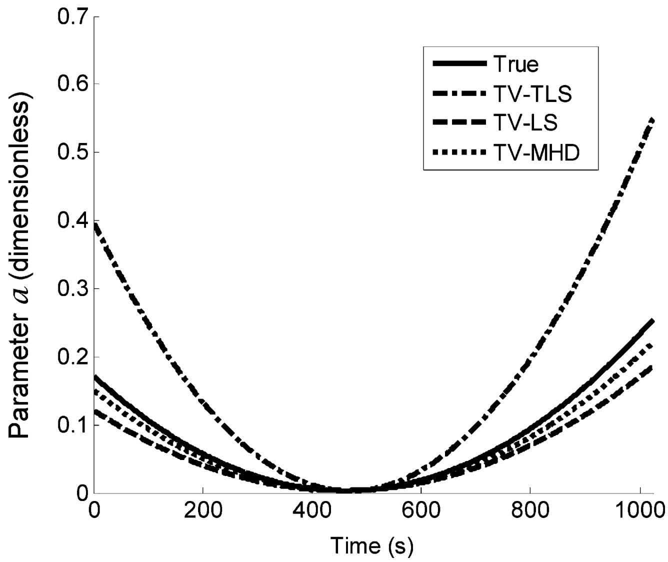


Fig. 4. Estimated value of the TV parameter "a" using the TVTLS, TVOPS, and TVMHD methods when "a" in (11) changes in a parabolic manner over time.

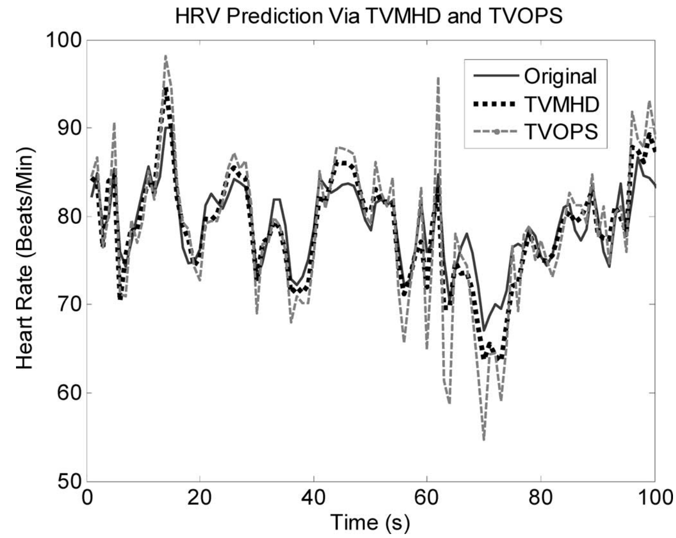


Fig. 5. Representative original (solid line) and the corresponding predicted HRV time series in the supine position via (dotted line) TVMHD and (dashed line) TVOPS methods.

TABLE IV
TIV COEFFICIENT ESTIMATES VIA TVOPS, TVTLS, AND TVMHD FOR SIMULATION EXAMPLE 3

| AR Model Coefficients | AR Terms | | |
|---|---|---|---|
| | **y(n-1)** | **y(n-2)** | **y(n-3)** |
| True value | -0.5 | -0.65 | 0.5 |
| TVOPS | -0.371±0.020 | -0.554±0.011 | 0.589±0.013 |
| TVTLS | -0.632±0.082 | -0.706±0.044 | 0.415±0.053 |
| TVMHD | -0.532±0.025 | -0.642±0.009 | 0.495±0.021 |

initial model was the same, but we used three Legendre basis functions, as this selection was the most appropriate, which was based on the NMSE criterion and given the fact that the dynamics change slowly. Similar to the previous two examples, the TVMHD provides the best accuracy in terms of the lowest NMSE value (fourth column of Table IV) by a factor of 3.6 and 14.6 to those of TVOPS and TVTLS, respectively. Consequently, the estimated TIV coefficient shown in Table IV and TV coefficient obtained by TVMHD are closest to the true values and the true TV parameter "$a$" shown in Fig. 4.

## *B. Application of TVMHD to Heart Rate Data*

In this section, we investigate the performance of TVMHD and TVOPS using human HRV time series. Using the model-order selection criterion, the TVOPS correctly selected only four significant model terms from our overdetermined model-order selection, as provided earlier. For the four significant terms, we found one nonlinear term in the condition encompassing both the supine and upright positions, and likewise, for the purely supine position. For the upright position, we found no nonlinear term. Fig. 5 shows a representative original (solid line) and the corresponding predicted HRV time series in the supine position via TVMHD (dotted line) and TVOPS (dashed line) methods. Note the better tracking of the HRV time series with TVMHD than TVOPS for all time points.

Table V shows the averaged NMSE values for all three conditions for each of the two selections of basis functions. As shown in Table V, we observe significantly lower NMSE values with the upright position when compared to either the supine or supine–upright positional change; the decrease is 64.8% when the upright position is compared to the supine positions using the TVOPS. The decrease in the NMSE value from the upright to supine–upright position is less, since some of the upright position data are included in the latter HRV time series. Our result is consistent with recent works, which suggest that nonlinearity seen in the supine position becomes less of a factor in the upright position [8]. For the supine position, we obtain a 17.9% decrease in the NMSE value with TVMHD when compared to TVOPS, whereas in the supine–upright position, this decrease is 15%. Note that because we only have linear terms in the upright position, the NMSE pertaining to TVMHD is essentially the same as the TVOPS. Further, it should be noted that for TVOPS, eight model terms were required to obtain similar NMSE values to those obtained via TVMHD, which only needed four terms. Therefore, TVMHD allows better representation of the true dynamics of the system even with a smaller number of model terms than TVOPS.

Increasing the number of Walsh basis functions from two to four, as shown in the third column of Table V, results in a significant decrease in the NMSE values only for TVOPS for the supine–upright condition. Note that the NMSE values obtained by TVMHD with only two Walsh and four Legendre basis functions are lower than those obtained with TVOPS with four Walsh and four Legendre basis functions especially during the supine position. Thus, our choice of the number of basis functions for these datasets was appropriate, as a further increase in the number of basis functions did not cause statistically significant reduction in the NMSE values. In addition, this result

TABLE V
AVERAGED NMSE VALUES FOR THE SUPINE–UPRIGHT, SUPINE, AND UPRIGHT POSITION VIA TVMHD AND TVOPS

| NMSE | | Selected model terms multiplied by the number of basis functions used | |
|---|---|---|---|
| | | **4 terms × (4L+2W)** | **4 terms × (4L +4W)** |
| Supine-upright | TVOPS | 0.283 ± 0.023 * | 0.248 ± 0.026 † |
| | TVMHD | 0.240 ± 0.027 | 0.222 ± 0.020 |
| Spine | TVOPS | 0.483 ± 0.041 * | 0.469 ± 0.038 |
| | TVMHD | 0.397 ± 0.034 | 0.378 ± 0.035 |
| Upright | TVOPS | 0.170 ± 0.019 * | 0.159 ± 0.022 |
| | TVMHD | N/A | N/A |

*Denotes that TVMHD provided significantly lower NMSE values than TVOPS in all body positions ($p < 0.05$) using Student $t$-test.

†Denotes that two additional Walsh basis functions did not significantly improve estimation accuracy except for TVOPS under the supine–upright data ($p < 0.05$). 4L+2W represents four Legendre and two Walsh basis functions.

TABLE VI
BASIS FUNCTION COEFFICIENT ESTIMATES FOR THREE SIMULATION EXAMPLES

| Simulation 1 | | Simulation 2 | | Simulation 3 | |
|---|---|---|---|---|---|
| $\left.\begin{matrix}\alpha_{110}\\ \underline{\alpha_{111}}\end{matrix}\right\} y(n-1)^2$ | 31.4766<br>$\underline{-0.8398}$ | $\left.\begin{matrix}\alpha_{110}\\ \underline{\alpha_{111}}\\ \underline{\alpha_{112}}\end{matrix}\right\} y(n-1)^2$ | -0.998<br>$\underline{1.986}$<br>$\underline{-25.3835}$ | $\left.\begin{matrix}\alpha_{110}\\ \underline{\alpha_{111}}\\ \underline{\alpha_{112}}\\ \underline{\alpha_{113}}\end{matrix}\right\} y(n-1)^2$ | -0.82073<br>$\underline{-2.42402}$<br>$\underline{-2.40677}$<br>$\underline{-7.1712}$ |
| $\left.\begin{matrix}\alpha_{10}\\ \underline{\alpha_{11}}\end{matrix}\right\} y(n-1)$ | -15.7231<br>$\underline{-0.0351}$ | $\left.\begin{matrix}\alpha_{10}\\ \underline{\alpha_{11}}\\ \underline{\alpha_{12}}\end{matrix}\right\} y(n-1)$ | -15.998<br>$\underline{0.04272}$<br>$\underline{-0.1241}$ | $\left.\begin{matrix}\alpha_{10}\\ \underline{\alpha_{11}}\\ \underline{\alpha_{12}}\\ \underline{\alpha_{13}}\end{matrix}\right\} y(n-1)$ | -15.928<br>$\underline{-0.11058}$<br>$\underline{-0.04572}$<br>$\underline{0.126956}$ |
| $\left.\begin{matrix}\alpha_{20}\\ \underline{\alpha_{21}}\end{matrix}\right\} y(n-2)$ | -20.5221<br>$\underline{-0.0258}$ | $\left.\begin{matrix}\alpha_{20}\\ \underline{\alpha_{21}}\\ \underline{\alpha_{22}}\end{matrix}\right\} y(n-2)$ | -20.801<br>$\underline{0.0308}$<br>$\underline{0.0896}$ | $\left.\begin{matrix}\alpha_{20}\\ \underline{\alpha_{21}}\\ \underline{\alpha_{22}}\\ \underline{\alpha_{23}}\end{matrix}\right\} y(n-2)$ | -20.8132<br>$\underline{-0.06006}$<br>$\underline{0.02681}$<br>$\underline{0.070813}$ |
| $\left.\begin{matrix}\alpha_{30}\\ \underline{\alpha_{31}}\end{matrix}\right\} y(n-3)$ | 16.1558<br>$\underline{-0.098}$ | $\left.\begin{matrix}\alpha_{30}\\ \underline{\alpha_{31}}\\ \underline{\alpha_{32}}\end{matrix}\right\} y(n-3)$ | 16.003<br>$\underline{0.02455}$<br>$\underline{-0.0634}$ | $\left.\begin{matrix}\alpha_{30}\\ \underline{\alpha_{31}}\\ \underline{\alpha_{32}}\\ \underline{\alpha_{33}}\end{matrix}\right\} y(n-3)$ | 16.048<br>$\underline{0.055578}$<br>$\underline{-0.02563}$<br>$\underline{-0.03643}$ |

TV alpha coefficient values (underlined) associated with a TV nonlinear term have large values as compared to linear TIV coefficients in three simulation examples. The first alpha coefficient (nonunderlined) represents TIV dynamics.

suggests that further reduction in the NMSE values with TVOPS is simply due to fitting eight additional parameters (increasing from two to four Walsh basis functions) and not due to capturing essential dynamics of the signal.

### C. Strategies for Reducing Computational Time

It should be noted that the greater accuracy of the TVMHD comes at the expense of significantly increased computational load. The computational time to compute a 300 data point HRV signal took four days for the TVMHD versus 1.17 s for the TVOPS using a 3GHz Intel Xeon microprocessor with a code written in MATLAB. The significant computing time required by the TVMHD is largely due to finding the minimum hypersurface distance among all possible combinations of the coefficient terms. Specifically, we assume that each coefficient is within $\pm 0.5$ of the initial estimated value. Thus, for each coefficient at an increment of $\pm 0.01$, we search for the minimal hypersurface distance among combination of all coefficients. With a greater number of terms, there will be a greater computational load, and thus, the TVMHD is applicable for systems that can be characterized by only a few parameters at present.

In most cases, we can increase the computational speed of the algorithm by assuming a certain SNR of the data or by making a tradeoff between improved accuracy and computation time. For example, we can limit the search space of the parameters to reduce the computational time. To illustrate this in more detail, our first simulation example employed (11), where the parameter $\alpha$

to be searched in (3) was varied within two different ranges: $\pm 0.25$ and $\pm 0.5$. The computational time for the $\pm 0.25$ range was 2 h, whereas it was three days for the $\pm 0.5$ range, and the NMSE values were 39.2% and 7.8%, respectively. Thus, limiting the search range can significantly reduce the computational time, but at the expense of reduced accuracy.

Another approach that we advocate to reduce the computational time is to recognize that any small $\alpha$ coefficients [e.g., all $\alpha_{1k}$, where $k > 0$ in (4)] that are representative of TV dynamics can be removed before the MHD minimization process of the algorithm. Note that $\alpha$ coefficients are estimated via TVOPS algorithm prior to the MHD minimization process. This approach serves two important functions. First, since the computational time is directly proportional to the number of $\alpha$ coefficients, eliminating those TV coefficients that have small value will significantly reduce the computational time. Indeed, in our first simulation example, such a procedure resulted in a significant reduction in computational time from three days to 5 h without significantly compromising the accuracy, as the NMSE increased to 9.9% from 7.8%. Second, values of $\alpha_{1k}$, where $k > 0$, allow us to discern which model terms are TV or TIV. For example, if the values of $\alpha_{1k}$ where $k > 0$ are nearly zero, then it can be assumed that these $\alpha$ coefficients are TIV. As shown in Table VI, the values of $\alpha_{1k}$, where $k > 0$, associated with the TV coefficients (underlined values) are significantly larger than those counterparts of TIV coefficients. In our application to HRV data, we note not only the inclusion of nonlinear terms in the supine position, but also many of the $\alpha_{1k}$, where $k > 0$, terms have large values (see Table VII). In the upright position, there was no nonlinear term and many of the $\alpha_{1k}$ where $k > 0$ terms have small values.

TABLE VII
BASIS FUNCTION COEFFICIENT ESTIMATES FOR HRV DATA FOR TWO POSTURAL POSITIONS

| Upright | | | Supine | | |
|---|---|---|---|---|---|
| $\alpha_{10}$ | $y(n-1)$ | 3.43055 | $\alpha_{110}$ | $y(n-1)^2$ | -2.3991 |
| $\alpha_{11}$ | | -1.52048 | $\alpha_{111}$ | | 27.1766 |
| $\vdots$ | | -1.43072 | $\vdots$ | | 14.5027 |
| | | -0.19829 | | | -6.1773 |
| | | 0.649407 | | | 11.5118 |
| $\alpha_{15}$ | | 3.412294 | $\alpha_{115}$ | | 15.1682 |
| $\alpha_{20}$ | $y(n-2)$ | 1.049922 | $\alpha_{10}$ | $y(n-1)$ | 14.7489 |
| $\alpha_{21}$ | | 0.07364 | $\alpha_{11}$ | | -0.7154 |
| $\vdots$ | | -1.55832 | $\vdots$ | | -0.1128 |
| | | -1.30322 | | | 0.8301 |
| | | -0.41686 | | | 2.2168 |
| $\alpha_{25}$ | | 0.279681 | $\alpha_{15}$ | | 1.6582 |
| $\alpha_{30}$ | $y(n-3)$ | -0.09536 | $\alpha_{20}$ | $y(n-2)$ | -1.9619 |
| $\alpha_{31}$ | | -0.53514 | $\alpha_{21}$ | | 1.5683 |
| $\vdots$ | | -1.50042 | $\vdots$ | | 0.4473 |
| | | 0.161719 | | | -2.3537 |
| | | 1.146857 | | | -1.7893 |
| $\alpha_{35}$ | | 0.8619 | $\alpha_{25}$ | | -0.2519 |
| $\alpha_{40}$ | $y(n-4)$ | 0.647311 | $\alpha_{30}$ | $y(n-3)$ | 1.0563 |
| $\alpha_{41}$ | | 0.199188 | $\alpha_{31}$ | | -0.2543 |
| $\vdots$ | | 0.419758 | $\vdots$ | | 0.495 |
| | | -1.21497 | | | 0.4002 |
| | | -0.56062 | | | 2.3064 |
| $\alpha_{45}$ | | -0.7241 | $\alpha_{35}$ | | 0.5326 |

TV alpha coefficients (underlined) associated with a nonlinear term in the supine position have large values as compared to linear coefficients in both supine and upright positions.

## IV. Discussion

We developed an algorithm that can model both nonlinearity and nonstationarity in data. The accuracy of the method was compared to an LS-based approach, namely, the TVOPS and TVTLS, and it was found that the proposed approach, the TVMHD, provides significantly more accurate results, as demonstrated with simulations and application to human HRV data. In simulation examples, we found the parameter estimates of TVMHD to be the closest to the true values and the NMSE values to be several orders of magnitude lower than those of the TVOPS and TVTLS. For HRV data in the supine position, we obtained similar NMSE values only when the number of parameters obtained by the TVOPS was two times greater than the number of TVMHD parameters.

The ability to obtain accurate and parsimonious parameter representation of the system dynamics facilitates numerous interesting options in the field of nonlinear system identification. For example, a given system can be characterized via a nonlinear AR model, and then, the coefficients can be used to determine if a given system exhibits behavior that is characteristic of deterministic chaos. The use of a TIV nonlinear AR model to characterize the behavior of nonlinear deterministic signals has been previously performed [9]. However, as it has been well documented in the literature [10], noise and TV dynamics can severely bias the detection of deterministically chaotic behavior of a system. More importantly, TV-based approaches for characterizing nonlinear deterministic behavior are currently lacking and the TVMHD approach fills that need.

Another potential application of the TVMHD is to develop a physiologically realistic model based on the coefficient estimates. While there have been many attempts to do so, successful outcomes have been limited because many of the approaches have relied on the use of the LS-based methods. As illustrated in this paper, the main problem is the attainment of many parameters and compounding the issue is the inaccurate parameter estimates with the LS-based methods. With fewer parameters required to accurately characterize the system dynamics as afforded by the TVMHD method, developing physiologically relevant block-structured models is now a distinct possibility. Furthermore, as our method is able to distinguish between TIV and TV dynamics, we can use our approach to test a hypothesis that a diseased system may have less nonlinear and TV dynamics than a healthy system.

The TVMHD method is a general method that can be applied to a wide variety of biological and physiological signals. While we illustrate in this paper the utility of the TVMHD in the form of a nonlinear AR model for HRV signals, the algorithm can be extended to multi-input and multi-output nonlinear ARMA models. Such an extension of the TVMHD would allow better

TABLE VIII
AR MODEL TERMS VIA TVMHD

| | **Supine** | **Upright** |
|---|---|---|
| Subject 1 | y(n-1); y(n-2); y(n-3); $y(n-3)^2$ | y(n-1); y(n-2); y(n-3); y(n-4); |
| Subject 2 | y(n-1); y(n-2); y(n-3); $y(n-1)^2$ | y(n-1); y(n-2); y(n-3); y(n-4); |
| Subject 3 | y(n-1); y(n-2); y(n-3); $y(n-1)^2$ | y(n-1); y(n-2); y(n-3); y(n-4); |
| Subject 4 | y(n-1); y(n-2); y(n-3); $y(n-2)^2$ | y(n-1); y(n-2); y(n-3); y(n-4); |
| Subject 5 | y(n-1); y(n-2); $y(n-2)^2$; y(n-3) | y(n-1); y(n-2); y(n-3); y(n-4); |
| Subject 6 | y(n-1); y(n-2); y(n-3); $y(n-1)^2$ | y(n-1); y(n-2); y(n-3); y(n-4); |

Note only linear model terms in the upright position, but inclusion of a nonlinear term in the supine position.

characterization of the cardiovascular control system by including other relevant signals, such as the blood pressure, respiration, stroke volume, cardiac output, and total peripheral resistance. However, a multiple signal representation with TVMHD is beyond the scope of the current paper, as the aim is to illustrate the novelty of the method in providing accurate and parsimonious representation of the system dynamics.

The absence of nonlinear model terms during the head-up tilt position, as seen in Table VIII, is in agreement with a study that used a TIV nonlinear method [11]. As shown in Table VIII, all six subjects' HRV dynamics are characterized consistently by the first four linear lag terms in the upright position. However, for the supine position, the fourth lag term that appears in all subjects during the upright position is replaced with a quadratic term, which has varying lag values among subjects. It should be noted that the compact model representation provided by TVMHD allows such discrimination of the difference in the model terms and captures a transition from nonlinear to linear dynamics as the body position changes from the supine to upright. The decreased complexity of the RR interval series in the head-up tilt position can be explained by the sympathetic activation induced by head-up tilt, which causes a rise in low-frequency oscillations and a drop in high-frequency oscillations, ultimately simplifying the dynamics of HRV [11].

While we can use the schemes outlined in Section III-C to reduce the computational time, the many hours of computational time required by the method, especially to achieve maximum accuracy, is a significant obstacle to overcome. However, with the ever-increasing computational speed of computers, the current problem of a large computational load with TVMHD may not be too much of a concern in the not-so-distant future.

## REFERENCES


[1] R. Zou, H. Wang, and K. H. Chon, "A robust time-varying identification algorithm using basis functions," *Ann. Biomed. Eng.*, vol. 31, pp. 840–53, Jul./Aug. 2003.

[2] M. Arnold, W. H. R. Miltner, R. B. H. Witte, and C. Braun, "Adaptive AR modeling of nonstationary time series by means of Kalman filtering," *IEEE Trans. Biomed. Eng.*, vol. 45, no. 5, pp. 553–562, May 1998.

[3] L. Faes, K. H. Chon, and G. Nollo, "A method for the time-varying nonlinear prediction of complex nonstationary biomedical signals," *IEEE Trans. Biomed. Eng.*, vol. 36, no. 2, pp. 205–209, Feb. 2009.

[4] L. J. Gleser, "Estimation in a multivariate "error in variables" regression model: Large sample results," *Ann. Statist.*, vol. 9, pp. 24–44, 1981.

[5] S. Lu and K. H. Chon, "Nonlinear autoregressive and nonlinear autoregressive moving average model parameter estimation by minimizing hypersurface distance," *IEEE Trans. Signal Process.*, vol. 51, no. 12, pp. 3020–3026, Dec. 2003.

[6] S. Lu, K. H. Ju, and K. H. Chon, "A new algorithm for linear and nonlinear ARMA model parameter estimation using affine geometry," *IEEE Trans. Biomed. Eng.*, vol. 48, no. 10, pp. 1116–24, Oct. 2001.

[7] K. H. Chon, H. Zhao, R. Zou, and K. Ju, "Multiple time-varying dynamic analysis using multiple sets of basis functions," *IEEE Trans. Biomed. Eng.*, vol. 52, no. 5, pp. 956–960, May 2005.

[8] M. J. Korenberg, "A robust orthogonal algorithm for system identification and time seris analysis," *Biol. Cybern.*, vol. 60, pp. 267–276, 1989.

[9] K. H. Chon, J. K. Kanters, R. J. Cohen, and N. H. Holstein-Rathlou, "Detection of chaotic determinism in time series from randomly forced maps," *Physica D: Nonlinear Phenom.*, vol. 99, pp. 471–486, Jan 1997.

[10] A, J. Theiler, S. Eubank, A. Longtin, B. Galdrikian, and J. D. Farmer, "Testing for nonlinearity in time series: the method of surrogate data," *Physica D: Nonlinear Phenom.*, vol. 58, pp. 77–94, Sep. 1992.

[11] A. Porta, S. Guzzetti, R. Furlan, T. Gnecchi-Ruscone, N. Montano, and A. Malliani, "Complexity and nonlinearity in short-term heart period variability: Comparison of methods based on local nonlinear prediction," *IEEE Trans. Biomed. Eng.*, vol. 54, no. 1, pp. 94–106, Jan. 2007.


**Bufan Yang** received the B.S. degree in biomedical engineering from Tsinghua University, Beijing, China, the M.S. degree in biomedical engineering from Stony Brook University, Stony Brook, NY. He is currently working toward the Ph.D. degree from the Department of Biomedical Engineering, Worcester Polytechnic Institute, Worcester, MA.

His current research interests include biosignal processing, physiological system identification, and understanding diabetic neuropathy using signal-processing approaches.

**Ki H. Chon** (SM'08) received the B.S. degree in electrical engineering from the University of Connecticut, Storrs, the M.S. degree in biomedical engineering from the University of Iowa, Iowa City, and the M.S. degree in electrical engineering and the Ph.D. degree in biomedical engineering from the University of Southern California, Los Angeles.

He is currently a Professor and the Chair of biomedical engineering at Worcester Polytechnic Institute, Worcester, MA. His research interests include medical instrumentation, biomedical signal processing, and identification and modeling of physiological systems.

Dr. Chon is currently an Associate Editor of the IEEE TRANSACTIONS ON BIOMEDICAL ENGINEERING.